



Article

Assessing the Potential of Hybrid Systems with Batteries, Fuel Cells and E-Fuels for Onboard Generation and Propulsion in Pleasure Vessels

Gianluca Pasini ¹, Filippo Bollentini ², Federico Tocchi ² and Lorenzo Ferrari ^{1,*}

¹ Department of Energy, Systems, Territory and Constructions, University of Pisa, 56122 Pisa, Italy; gianluca.pasini@unipi.it

² Sanlorenzo S.p.a., 19126 La Spezia, Italy; f.bollentini@sanlorenzoyacht.com (F.B.); f.tocchi@sanlorenzoyacht.com (F.T.)

* Correspondence: lorenzo.ferrari@unipi.it

Abstract: Electro-fuels (E-fuels) represent a potential solution for decarbonizing the maritime sector, including pleasure vessels. Due to their large energy requirements, direct electrification is not currently feasible. E-fuels, such as synthetic diesel, methanol, ammonia, methane and hydrogen, can be used in existing internal combustion engines or fuel cells in hybrid configurations with lithium batteries to provide propulsion and onboard electricity. This study confirms that there is no clear winner in terms of efficiency (the power-to-power efficiency of all simulated cases ranges from 10% to 30%), and the choice will likely be driven by other factors such as fuel cost, onboard volume/mass requirements and distribution infrastructure. Pure hydrogen is not a practical option due to its large storage necessity, while methanol requires double the storage volume compared to current fossil fuel solutions. Synthetic diesel is the most straightforward option, as it can directly replace fossil diesel, and should be compared with biofuels. CO₂ emissions from E-fuels strongly depend on the electricity source used for their synthesis. With Italy's current electricity mix, E-fuels would have higher impacts than fossil diesel, with potential increases between +30% and +100% in net total CO₂ emissions. However, as the penetration of renewable energy increases in electricity generation, associated E-fuel emissions will decrease: a turning point is around 150 gCO₂/kWhel.

Keywords: E-fuel; fuel cell; lithium batteries; hybrid system; pleasure vessel; efficiency; storage volume; CO₂ emissions



Citation: Pasini, G.; Bollentini, F.; Tocchi, F.; Ferrari, L. Assessing the Potential of Hybrid Systems with Batteries, Fuel Cells and E-Fuels for Onboard Generation and Propulsion in Pleasure Vessels. *Energies* **2024**, *17*, 6416. <https://doi.org/10.3390/en17246416>

Academic Editor: JongHoon Kim

Received: 25 November 2024

Revised: 12 December 2024

Accepted: 18 December 2024

Published: 20 December 2024



Copyright: © 2024 by the authors. Licensee MDPI, Basel, Switzerland. This article is an open access article distributed under the terms and conditions of the Creative Commons Attribution (CC BY) license (<https://creativecommons.org/licenses/by/4.0/>).

1. Introduction

In recent years, there has been a growing emphasis on reducing pollutants and climate changing emissions from all human activities, including the maritime sector. The International Maritime Organization (IMO) has implemented regulations to curb emissions of nitrogen oxides (NO_x) and sulfur oxides (SO_x) [1] and is setting an ambitious target of a 50% reduction in greenhouse gas emissions by 2050 compared to 2008 levels [2].

In tandem with the escalating focus on sustainable practices in luxury yachting, stakeholders are setting ambitious emission reduction targets. Notably, the International Maritime Organization's MEPC, under the Marpol Annex VI amendments, has outlined a phased approach towards a substantial reduction in carbon emissions. Initial targets aim for a 40% reduction in greenhouse gas (GHG) emissions by 2030 compared to 2008 levels, with a subsequent goal of a 70–80% reduction by 2040 and net zero by 2050 [3]. These quantitative benchmarks serve as a catalyst for innovation and investment in alternative propulsion systems, including synthetic fuels. In line with these broader maritime emission reduction efforts, the pleasure boat sector must carefully account for its environmental impact. Typically, luxury yachts are equipped with high-speed diesel engines powered by marine diesel oil (MDO). Pleasure vessels above 24 m in length and falling under 500 gross

tonnage (GT) often utilize multiple internal combustion engines of different sizes, fueled with fossil diesel, to fulfill propulsion and onboard electricity generation requirements.

Many researchers have studied onboard microgrids and their demanding specifications in terms of power and intermittent energy production patterns [4,5]. Furthermore, shipboard microgrids in modern pleasure boats are constrained by stringent volume limitations, hindering the integration of different electricity generation systems and storage solutions [6]. Hybrid propulsion and service load systems for vessels typically involve a diesel generator coupled with lithium-ion batteries. Some studies have shown that such systems can achieve fuel savings of approximately 7% compared to conventional layouts [7]. Some studies have explored fuel cells powered by hydrogen generated onboard through steam methane reforming of liquified natural gas (LNG) [8,9], demonstrating that the primary driver of CO₂ reduction is the fuel substitution, not the generation devices themselves. Renewable energy sources (RESs) such as solar and wind power are inherently intermittent and unpredictable, posing challenges in their consistent and stable utilization. Future mobility (road, air and water) represents a new electrical load (for battery recharging or E-fuel production) [10,11] that could help RES utilization.

The maritime and waterborne sector, which lags behind other sectors in decarbonization efforts, in recent years made progress in many aspects, such as optimizing electrical consumption, hull design and antifouling coatings to reduce GHG emissions. However, in the future, this sector can hypothetically reap significant benefits from the decarbonization of electricity generation through two main approaches: direct electrification with battery electric systems (and direct power supply during port docking) or the utilization of fuels produced with electricity (E-fuels). Large ships cannot be totally electrified with batteries because the power and energy demands are too large. Other options must be considered since currently there is not a clear winning solution [12].

This study moves from a review of E-fuels and their synthesis and then investigates different layouts for generation and propulsion based on different E-fuels. Fuel cell and internal combustion engines fueled with methanol, hydrogen and synthetic diesel, in combination with batteries, are compared in terms of efficiency, emissions and volume/mass requirements.

2. Comparison of E-Fuels, from Synthesis to Final Use

2.1. Hydrogen

Hydrogen is the smallest and lightest element on the periodic table, forms the lightest stable molecule (H₂) and is a gas at ambient conditions. It is colorless, odorless and non-toxic. Its self-ignition temperature is similar to that of natural gas. The flammability range is 4–75% [13], which is very wide compared to other fuels, while the energy required to start the combustion reaction is similar to that of other fuels at low concentrations but much lower at higher concentrations. The lower calorific value of hydrogen is 33.3 kWh/kg, the highest among all fuels, considering its density of 0.084 kg/Sm³, and the lower volumetric calorific value equals 2.8 kWh/Sm³.

Hydrogen can be synthesized starting from electricity and water through electrolysis. Alkaline electrolyzers are the most widespread on the market; PEM electrolyzers are under development, with the first models now commercialized [14], while high-temperature electrolyzers are still in the research stage [15]. The conversion efficiency of the technologies currently in use is around 60–80% (based on HHV); therefore, the specific consumption is around 49–65 kWh/kg. A more realistic range can be 50–55 kWh/kg [15,16].

Hydrogen is transported at pressures around 200–250 bar, while 700 bar tanks are already available. The energy consumption required to compress hydrogen to 700 bar is 5.3–6 kWh/kg [17,18]. The density of hydrogen at such pressure and ambient temperature is 40 kg/m³, while the energy density is 1.3 kWh/L. At 350 bar, instead, the density is 27 kg/m³, with an energy density that drops to 0.9 kWh/L; in this case, the work required for compression is about 4.6 kWh/kg [19].

Hydrogen can be liquefied, in which case the energy consumed by the process is approximately 10–15 kWh/kg [17,18]. Low temperatures require the use of well-insulated

cryogenic tanks; therefore, their volume increases. The density of liquid hydrogen is 71 kg/m^3 , so the energy density is 2.3 kWh/L .

Hydrogen can be used for onboard energy conversion in fuel cells (FCs) and internal combustion engines (ICEs); PEMFCs are particularly interesting due to their reduced startup time and acceptable modulation range, with efficiencies estimated around 40–60%. Power density and lifespan could be critical for some applications, and performance degradation during operation limits their commercialization, making accurate prediction essential. However, reversible voltage loss recovery during operation complicates model training and prediction [20].

Regarding ICEs, the use of hydrogen has been studied with great interest in recent decades. Many prototypes have been developed and tested, showing an efficiency comparable to that of diesel ICEs [21–23].

2.2. Methanol

Methanol (CH_3OH) is currently produced almost entirely from fossil fuels. It is used in the production of formaldehyde, from which plastics and coating products are obtained; it is also used in the oil and gas industry [24]. Its molar mass is 32.04 g/mol , and its lower calorific value is 19.9 MJ/kg , or 5.5 kWh/kg . In ambient conditions, it is in a liquid state and its density is 796 kg/m^3 , so its energy density is 4.4 kWh/L .

Methanol can be produced from hydrogen and carbon dioxide. In Iceland, there is a plant that produces methanol using electrolytic hydrogen and CO_2 recovered from geothermal power plants, and it has an efficiency of 41.9% (with reference to the lower calorific value) [25]. The efficiency of the entire process is mainly driven by the production of hydrogen. Other sources indicate an efficiency of 53–57% [21,26]. To produce 1 kg of methanol, 1.37 kg of CO_2 and 0.19 kg of H_2 are needed.

Methanol can be used as fuel for two-stroke diesel or four-stroke Otto cycle internal combustion engines. In the first case, there is a model produced by MAN (MAN ME-LGI) used in tankers powered with this fuel. As for four-stroke engines, a Wärtsilä model is in use on the Stena Germanica ferry [21].

Another possibility is the adoption of fuel cells. Between Helsinki and Stockholm, the ferry MS Mariella operates with fuel cells powered by methanol. These have a low efficiency, around 20%, and are still under development [27]. Fuel cells can be powered by hydrogen produced by methanol steam reforming, and the efficiency of this process is around 50–75% [28,29]. Normal PEMFCs (operating at 60–90 °C) or high-temperature PEMFCs (operating at 120–200 °C) can be used if the reforming stage produces high-temperature hydrogen. However, in this study, low-temperature PEMFCs are considered due to their higher technology maturity and fewer safety implications.

2.3. Ammonia

Ammonia is currently produced worldwide almost entirely from fossil fuels, and it is mainly used in the production of fertilizers [30]. Its molar mass is equal to 17.03 g/mol , and in ambient conditions it is a vapor. The lower heating value is 18.6 MJ/kg , or 5.2 kWh/kg . The density of liquid ammonia at 10 bar and ambient temperatures is about 610 kg/m^3 ; therefore, its energy density is 3.2 kWh/L . The European Union sets ammonia exposure limits of 20 ppm for 8 h and 50 ppm for 15 min. Exposure to larger amounts of ammonia can lead to lung damage and death. It is very water soluble, so it is easily absorbed by body fluids such as saliva, tears and sweat.

Ammonia production relies on the well-known Haber–Bosch process, in which hydrogen, usually produced by natural gas reforming, reacts with nitrogen at 450 °C and 200 bar in the presence of an iron-based catalyst [31]. The production of green ammonia, based on electrolytic green hydrogen, showed an efficiency of 50–52% with the technologies currently used [31,32]. To produce 1 kg of ammonia, 0.18 kg of H_2 and 0.82 kg of N_2 are needed. Scientific research is currently focused on the possibility of using solid oxide electrolyzers

at higher temperatures to recover thermal energy from the reactor of the synthesis process. For this type of plant, an efficiency up to 71–74% is estimated [32,33].

Ammonia, like methanol, can be used in two- or four-stroke internal combustion engines. In recent decades, studies have been conducted mainly on small displacement engines for automotive use [32]. Regarding fuel cells, low-temperature PEM must be powered by pure hydrogen; therefore, it is necessary to carry out cracking of ammonia, which can consume at least 14% of the demand for thermal energy [31]. Solid oxide fuel cells can be fed directly to ammonia [31].

2.4. Synthetic Diesel

Diesel is a fuel that is in a liquid state in ambient conditions; its density is 850 kg/m^3 , and its lower calorific value is about 43 MJ/kg . So, the energy density is 36.6 MJ/L , or 10 kWh/L .

This fuel can be synthesized from hydrogen and CO_2 by the Fischer–Tropsch process, whose efficiency is estimated at around 75% [21]. The power-to-fuel efficiency to produce synthetic diesel is around 51–53% [21–34].

Synthetic diesel can be used in compression–ignition internal combustion engines. In the field considered in this study, four-stroke fast engines are used. It is a well-known fuel, and the whole industrial sector has strong experience with its distribution and use.

2.5. Synthetic Methane

Methane in ambient conditions is in a gaseous state, and its lower calorific value is 13.9 kWh/kg ; however, its density is low, 0.67 kg/Sm^3 in standard conditions, which brings the volumetric calorific value to 9.3 kWh/Sm^3 .

Methane synthesis is carried out using the Sabatier process, whose efficiency is around 75% [21]. The power-to-fuel efficiency is around 50–65% [34]. Methane storage can also be in liquid form at $-161 \text{ }^\circ\text{C}$; therefore, cryogenic tanks are required. The density of liquid methane is around 426 kg/m^3 , so the energy density becomes 5.9 kWh/L . The efficiency of the liquefaction process is very high, more than 90% [21].

Methane can be used in spark-ignition internal combustion engines. Solid oxide and molten carbonate fuel cells can be fueled directly by methane, while others require hydrogen. This can be produced directly onboard by steam methane reforming [35].

2.6. E-Fuel Comparisons

A comparison of E-fuels based on their energy density can be found in Figure 1 [10,36,37]. Containment must be taken into account for a real application like luxury yachts.

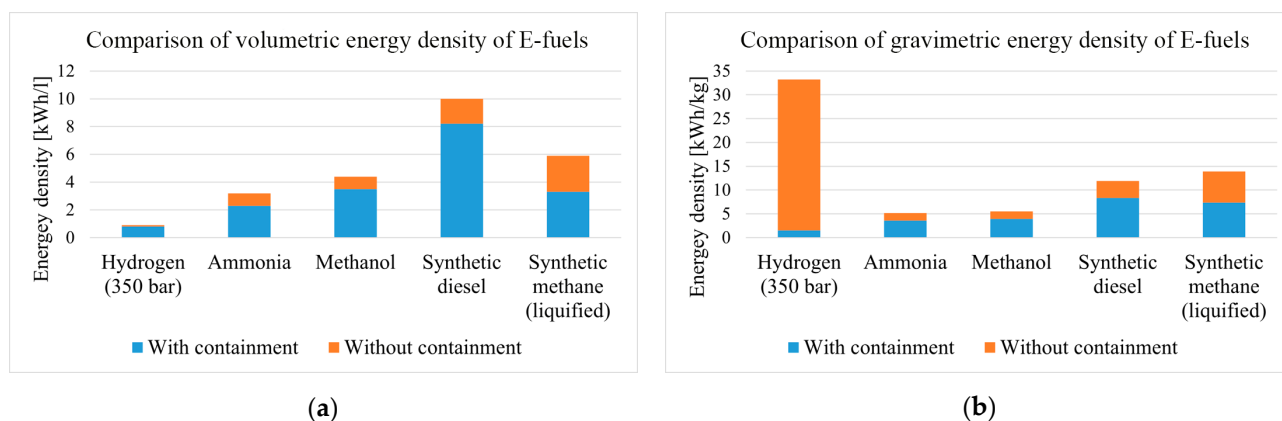


Figure 1. A comparison of volumetric (a) and gravimetric (b) energy densities of E-fuels [10,36,37].

Considering a future scenario where low-emission electricity is available, different pathways of E-fuels from an energetic point of view can be compared. The steps considered in this analysis are production, distribution and energy generation for final use. For each phase, a range of energy efficiency is estimated.

Another important consideration is related to the most suitable fuel cell technology: considering the possibility of frequent start–stop and power modulation, the best choice is the PEM fuel cells. PEMs can only use pure hydrogen as fuel, making the onboard conversion of methane, ammonia and methanol (cracking or steam reforming) mandatory.

Liquid hydrogen, despite its advantages regarding energy density, requires the use of complex extreme cryogenic technologies that are completely extraneous to the maritime industry; its use has a very low technology readiness level, currently used only in few research activities. For these reasons, hydrogen is evaluated only in gaseous form at 350 bar.

The innovative processes of ammonia synthesis with heat recovery have only been hypothesized; there are no real applications. Moreover, these approaches require high-temperature electrolyzers, which are more suitable for constant operation over time than for electricity networks with a high installed capacity of renewable energy sources. Therefore, only standard ammonia production processes are considered. The results are shown in Table 1.

Table 1. Comparison of efficiencies in supply chains and onboard usage of E-fuels.

E-Fuel	Production	Distribution	Onboard Usage	Power-to-Power
Hydrogen	51–67% [15,16]	82–86% [17–19]	30–60% [21–23]	13–35%
Methanol	42–57% [21,25,26]	50–75% [28,29]	35–60% [21–23]	8–26%
Ammonia	50–52% [31,32]	85% [31]	30–60% [21,31,32]	17–31%
Synthetic diesel	51–53% [21,34]	-	35–45% [21]	18–24%
Synthetic methane	50–65% [34]	46–77% [21,35]	35–60% [21–23]	9–30%

This section can be concluded by acknowledging the absence of a clear winner in the comparison if based only on energy efficiency. The complete evaluation of these options must be technological, economic and cover other aspects, such as design, volume and weight impacts. The interest of the pleasure vessels' industry in methanol is rapidly increasing, thanks to its decent energy density (liquid form in ambient conditions), with acceptable volume and weight requirements and also a manageable refueling operation. Instead, the energy sector in general is more focused on pure hydrogen because it has the simplest production chain without any additional synthesis reactor. Since this study is focused specifically on the yachting sector, only these two energy vectors (hydrogen and methanol) were considered, together with diesel, which is useful to compare all the options in the current situation and to analyze the possible replacement with synthetic diesel.

3. Case Study and Methodology

The case study analyzed is based on a 50 m luxury pleasure boat produced by Sanlorenzo spa company; it is equipped with two 118 kW diesel gensets to generate electricity and two 969 kW diesel ICEs for propulsion. To simulate the alternative configurations, data provided by the company regarding the electrical load onboard and the speed of the boat were used. The period of a single trip (port-to-port) considered is 15 days. Data on electricity consumption onboard were available, and sampling was carried out every 30 s; the resolution was 1 kW. This consumption is due to equipment such as air conditioning, boilers, bow thrusters, etc. In the code, developed in a Matlab (R2021) environment, the data were reduced, bringing the resolution to 1 min, because shorter dynamics are out of the scope of the study. Data on the boat speed were available, with one sample per hour. To exclude insignificant maneuvering phases, only values above 5 knots were considered.

3.1. Simulated Configurations

In this section, the alternative configurations that were analyzed during the simulation phase are described. The base case, with diesel engines and gensets, is the reference case. In other configurations, innovative technologies were introduced, such as hydrogen-powered fuel cells and a methanol steam reformer. All electricity production systems include a

lithium battery pack, which is used for peak shaving and allows for the reduction of the size of generation devices. All the configurations are in Table 2.

Table 2. Analyzed configurations.

Configurations	Electricity Generation/Propulsion	Description
Synthetic diesel ICE	Synthetic diesel genset Synthetic diesel engines	Present time conditions and technologies
Synthetic diesel–methanol ICE-FC	FC with methanol reformer Synthetic diesel engines	While the boat is moving, the FC is shut down and electric generation is powered by the main engines
Synthetic diesel–hydrogen ICE-FC	Hydrogen FC Synthetic diesel engines	While the boat is moving, the FC is shut down and electric generation is powered by the main engines
Hydrogen FC	Hydrogen FC Electric motors	Electricity generation is only carried out with FCs; propulsion is purely electric
Methanol ICE	Methanol genset Methanol engines	Methanol is compatible with current technologies (ICEs)

3.2. Methodology

Simulations are carried out on the considered 15-day trip, supplying electrical load and boat propulsion. These calculations are repeated by varying the capacity of the battery pack and the size of the onboard electricity generation system. The output results cover various aspects: consumption, dimensions, CAPEX and CO₂ emissions.

The size of the propulsion engines is chosen to reach the target maximum speed; in the case of electric propulsion with hydrogen FCs, the same method is applied. As for onboard electricity generation, the sizes of the genset or FC system and the capacity of the battery pack used in the simulations are as follows:

- The capacity of the batteries (C_{st}) varies from 0 kWh to 400 kWh, with a step of 25 kWh.
- The nominal power of the fuel cell varies from a minimum of 90% of the average load, i.e., 57 kW to 200 kW. This is carried out with the hypothesis of being able to soon have many models on the market of many sizes (currently, only a few are available).
- The power of the diesel genset varies from 110% of the maximum load, i.e., 142 kW, to 90% of the average load, 57 kW.

Finally, the results of some configurations of particular interest are further deeply compared: as far as fuel cells are concerned, real models are considered to see the results that can be obtained with the models currently on the market. Configurations with FCs of 70–80 kW and 200 kW are analyzed to simulate the adoption of real models produced by Toyota, Ballard or Powercell. As for internal combustion generators, the power size is also varied, an evaluation that is more realistic for this technology thanks to the numerous models on the market. At the end of the simulations, we focus on two sizes of gensets: one that allows the load to be satisfied independently, and another less powerful one that is assisted by a battery pack. For the propulsion load in the case of fuel cells, it is assumed to implement a group of ten cells of 200 kW, reaching a total power similar to that of the ICEs. To compute the consumption of electricity generation, correlations of specific consumption and load factors are used for gensets and FCs; as for propulsion, the speed–break power curve of the boat provided by the company is used.

CAPEX is estimated by using real data provided by the company and its suppliers:

1. For the fuel cell system, 4000 EUR/Kw;
2. For the fuel cell system with a reformer, 6000 EUR/kW;
3. For battery packs, 750 EUR/kWh;
4. The cost of the two engines for propulsion is 500 kEUR;
5. The cost of the generators is estimated knowing that of three specimens of different sizes (EUR 40,000 for a nominal power of 60 kW, EUR 54,000 for 118 kW and EUR 56,500 for 150 kW).

Some of these values are higher than other sector ones, indicating also that marinization and small volumes have a remarkable impact on costs.

The volume and weight of tanks and engine room components are evaluated with the parameters in Table 3 [36,37].

Table 3. Data about dimensions of components and tanks [36,37].

Technology	Engine Room Components	
	Gravimetric Power Density [W/kg]	Volumetric Power Density [W/L]
Diesel genset	60	50
Diesel engine	420	370
Fuel cell system	200	100
Reformer	80	35
Energy Vector	Fuel Tanks	
	Gravimetric Energy Density [kWh/kg]	Volumetric Energy Density [kWh/L]
Hydrogen (350 bar)	1.5	0.8
Methanol	3.9	3.5
Diesel	8.3	8.2

In the following sections, a comparison of CO₂ emissions is carried out: it is extremely important considering the carbon intensity of electricity used to produce synthetic fuels used onboard.

3.3. Control Logic

The methanol reformer has a limited modulation range, just 1 kW/min, while the hydrogen FC can reach 10 kW/min. Considering the fluctuations in the time of electric load, a control logic that keeps the state of charge (SoC) of the battery pack at a desired value, while being compatible with the FC's modulation range, is needed. Moreover, it is important to consider that the power output of the reformer should be as constant as possible to guarantee a longer lifetime of the component.

The solution used in this case is a proportional–integral control with a low-pass filter: first, the value of P_{set1} is computed with the formula below.

$$P_{set1}(t) = P_{avg}(t) + K_P \cdot e(t) + K_I \cdot \sum_{i=t-n}^t e(i) \quad (1)$$

P_{avg} is the moving average of the electric load computed in the previous n timesteps, K_P is the proportional constant, K_I is the integral constant and e is the error signal:

$$e(t) = SoC(setpoint) - SoC(t - 1) \quad (2)$$

After calculating the value of P_{set1} , it is corrected so that it respects the required modulation range and does not exceed the maximum power. Finally, the power delivered by the fuel cell P_g is calculated, introducing constraints on battery capacity ($SoC_{max} = 0.95 C_{st}$; $SoC_{min} = 0.2 C_{st}$) and the maximum charging and discharging power, P_c and P_d , respectively, both equal to 1 C.

If the battery is charging

$$SoC(i) = SoC(i + 1) + \min \left[(P_{set1}(i) - L(i)) \cdot \Delta t; (SoC_{max} - SoC(i - 1)) \cdot \frac{C_{st}}{\eta_c}; P_c \cdot \Delta t \right] \cdot \frac{\eta_c}{C_{st}} \quad (3)$$

If the battery is discharging

$$SoC(i) = SoC(i - 1) + \min \left[(L(i) - P_{set1}(i)) \cdot \Delta t; (SoC(i - 1) - SoC_{min}) \cdot \frac{C_{st}}{\eta_d}; P_d \cdot \Delta t \right] \cdot \frac{\eta_d}{C_{st}} \quad (4)$$

where η_c and η_d are the charging and discharging efficiencies of batteries, respectively, both equal to 0.95. n is the number of timesteps on which the moving average and the integral component of the control are calculated. The greater this window of time, the more the signal trend will be smooth and soft; however, the lag between electric load and the moving average will also increase. Therefore, a compromise must be found between these two aspects. Fast Fourier transform of the electric load curve was used to acknowledge which were the most important frequencies; it turned out that there is a peak in a 9–10 min period, so n should be the same or one multiple. Moreover, following the procedure shown in [38], the sum of absolute differences for different window sizes was calculated. Increasing this window, the sum of absolute differences must rise until it stabilizes; this means that the moving average calculated beyond a certain time range does not bring further significant advantages in making the trend smoother. Therefore, the point at which this stabilization begins can be a good value for choosing n . In the end, a time window of 30 min was chosen. These elaborations can be seen in Figure 2.

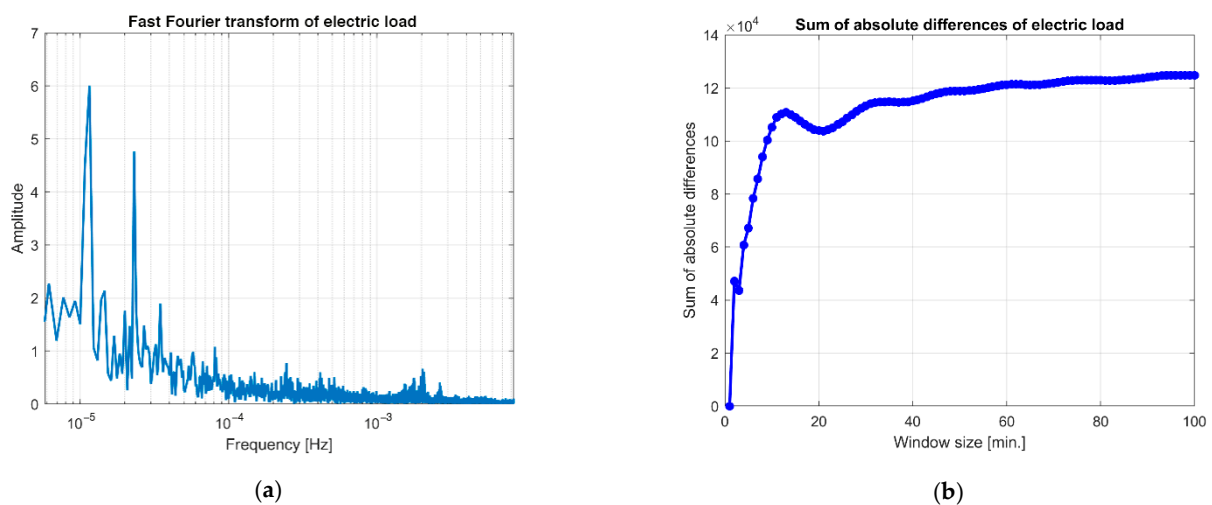


Figure 2. Fast Fourier transform of electric load (a) and sum of absolute differences of electric load with different window sizes (b).

To choose the values of K_P and K_I , it is necessary to find a trade-off between the smoothness of power production and the respect of the SoC setpoint following. Simulations of an FC, methanol reformer and battery system are carried out in Matlab (R2021) by varying the values of K_P and K_I . Firstly, the total energy produced by the FC and the total deficit of the system are considered: the first aspect is not greatly influenced by the values of K_P and K_I , so all cases are similar from this point of view; as for the total deficit, it is zero if K_I is less than 0.27, and, in fact, the green dashed line in the following figures separates the configurations with a deficit from those without it. The parameters computed in these simulations that seem to be the most useful for this purpose are as follows:

- The standard deviation of the power generated by the fuel cell: this is an index of the softness of the control system, and it must be minimized.
- The sum of absolute differences of the power generated by the fuel cell: this is also an index of the softness of the control system; therefore, it must be as small as possible.
- The setpoint index: the number of timesteps in which the SoC is around the set setpoint, considering a range of $\pm 1\%$; it indicates the effectiveness of the control on the state of charge, and it must be maximized.
- The maximum SoC reached: a very high value of the maximum SoC can bring the system into saturation; this is not desirable, so it must be minimized.

The standard deviation and the sum of the absolute differences of the power delivered by the fuel cell, present in Figure 3, assume lower values if K_P and K_I are smaller. It is

important to note that these two parameters should be minimized, if possible, because of the importance of the smoothness of the FC’s power delivery.

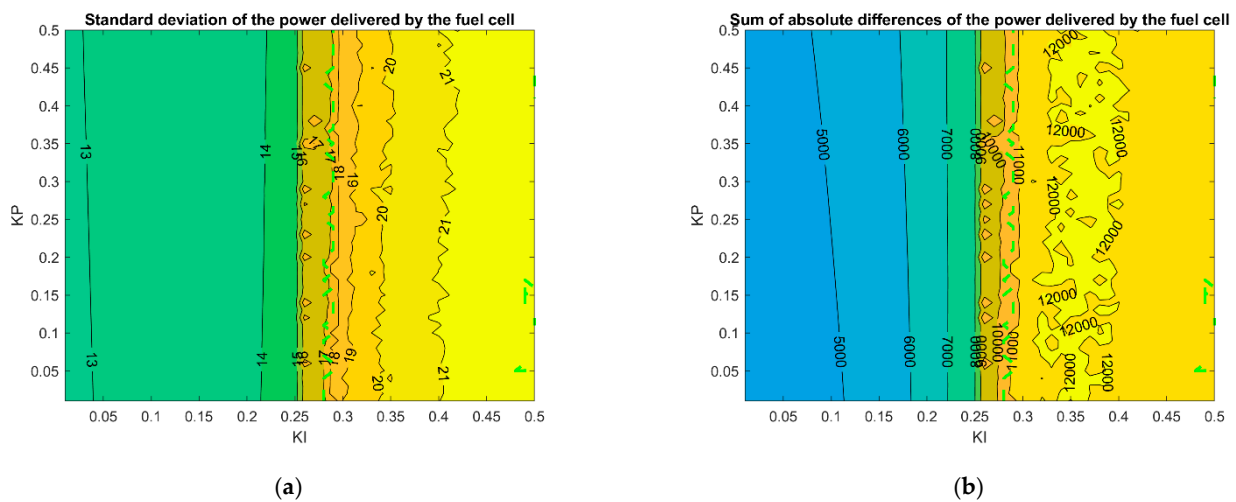


Figure 3. Standard deviation (a) and the sum of absolute differences (b) of the power delivered by the fuel cell with different values of K_P and K_I .

Battery SoC estimation is another important aspect that is not analyzed here in detail. A good estimation enables users to optimize usage strategies, maintaining safe charging and discharging ranges to prevent structural damage to active materials and capacity degradation. Accurate SoC estimation, especially in fluctuating temperatures, is vital to mitigating risks like thermal runaway and ensuring reliability [39].

Regarding the setpoint index, shown in Figure 4, it becomes higher if the values of the constants of the control system are low. In this case, higher values of the parameter are preferred: the setpoint index shows if the control system manages to keep the SoC at the setpoint value. The maximum SoC reached, shown in Figure 4, instead becomes lower with small values of K_P and K_I ; this parameter should be minimized, because if it is low, it means that the response of the system is smooth and gradual, while at the same time, it is important not to reach excessively high SoC values, which can bring saturation of the system.

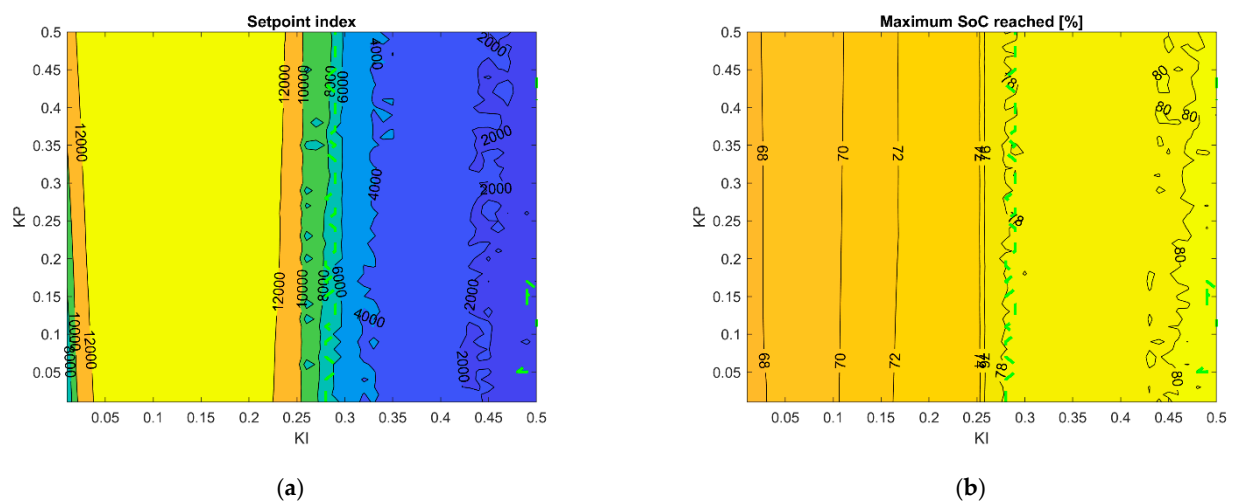


Figure 4. Set-point index (a) and maximum SoC (b) reached with different values of K_P and K_I .

It seems that the values of K_P and K_I should be lower than 0.2 but higher than 0.04. Before choosing the values to use in the following simulations, it is important to underline

that the graph of the operation of the system in the time and the histogram of the power output of the FC have also been taken into account; however, there are many combinations of K_P and K_I that guarantee the correct operation of the system. After these considerations, the following values were chosen: $K_P = 0.08$ and $K_I = 0.05$.

In the configurations in which there are both FCs and diesel engines with generators, when the boat is moving, the FC is shut down and generators are used to produce electricity. In this case, the maximum charging and discharging power is limited to $0.3 \cdot C_{st}$ in order to charge the battery pack slowly, while the FC is reducing its power output; this is useful to avoid saturation of the system.

Regarding the genset and battery system, the power modulation range of conventional gensets is adequate; moreover, their efficiency increases with higher load factors, so in this case, a simpler control system can be used. At each timestep, SoC is computed, using the power P_g of the genset and electric load L as inputs.

If the battery is charging

$$SoC(i) = SoC(i + 1) + \min \left[(P_g(i) - L(i)) \cdot \Delta t; (SoC_{max} - SoC(i - 1)) \cdot \frac{C_{st}}{\eta_c}; P_c \cdot \Delta t \right] \cdot \frac{\eta_c}{C_{st}} \quad (5)$$

If the battery is discharging

$$SoC(i) = SoC(i - 1) + \min \left[(L(i) - P_g(i)) \cdot \Delta t; (SoC(i - 1) - SoC_{min}) \cdot \frac{C_{st}}{\eta_d}; P_d \cdot \Delta t \right] \cdot \frac{\eta_d}{C_{st}} \quad (6)$$

4. Results

The simulation of the synthetic diesel ICE configuration shows that the addition of batteries causes a high increase in the CAPEX, with a very low reduction in consumption, achieved by making the generator work with higher load factors. The system with an 80 kW generator and 75 kWh battery leads to a 5% reduction in consumption compared to the basic case with a 142 kW genset without batteries, while the cost increases by 93%. A positive point of adding accumulators is the reduction in volume by 13%. These results are shown in Figure 5. Similar considerations can be made for the methanol ICE configuration, the results of which are in Figure 6.

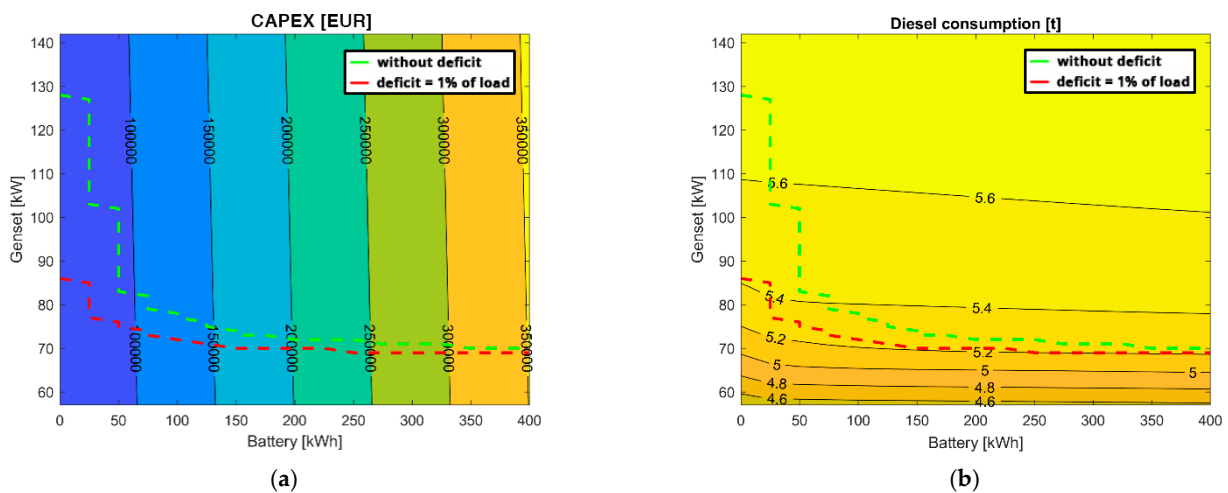


Figure 5. CAPEX (a) and diesel consumption (b) of electricity production system of the configuration diesel ICE.

The synthetic diesel-methanol ICE-FC configuration, in the part of the electricity generation system, shows that the addition of batteries and the reduction in the size of the fuel cell allows to reduce the CAPEX and the size. Consumption, on the other hand, increases, because the fuel cell tends to work with higher load factors, in which the efficiency is lower. The combination with the 70 kW fuel cell and 175 kWh battery, compared to

that with the 200 kW fuel cell and 100 kWh battery, reduces the cost by 57% and volume by 13%, and methanol consumption increases by 20%. It can also be seen that synthetic diesel consumption related to electricity production by alternators increases slightly with larger-capacity batteries, as is to be expected. The data of this configuration are in Figure 7.

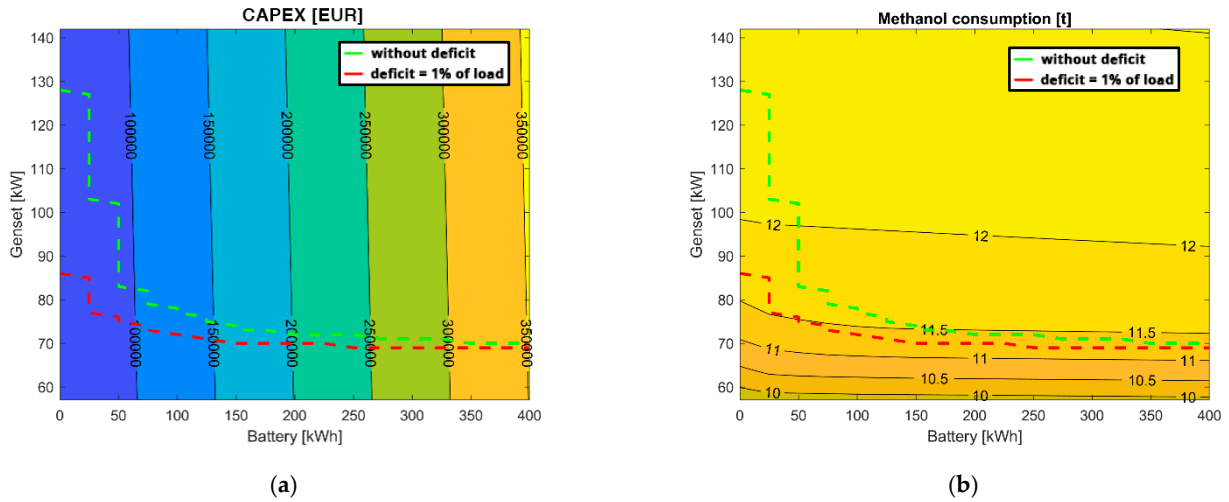


Figure 6. CAPEX (a) and methanol consumption (b) of electricity production system of the configuration methanol ICE.

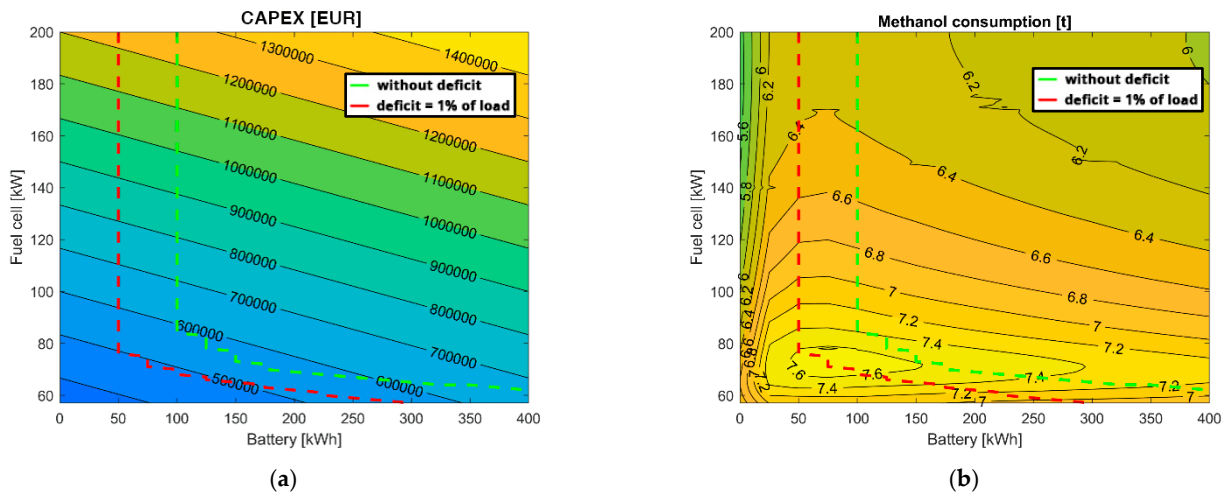


Figure 7. CAPEX (a) and methanol consumption (b) of electricity production system of the configuration diesel-methanol ICE-FC.

The synthetic diesel-hydrogen ICE-FC configuration leads to results similar to the previous one in terms of the CAPEX and consumption trends, while the volume tends to increase with smaller fuel cells due to the larger footprint of the hydrogen tanks for higher consumption and the absence of the reformer, a very bulky component. The configuration with a 70 kW fuel cell and 175 kWh battery, compared to that with a 200 kW fuel cell and 75 kWh battery, has 23% higher hydrogen consumption, a cost 52% lower, while the volume increases by 18%. These results can be seen in Figure 8.

Regarding electricity production, the hydrogen FC configuration shows similar trends to the previous one, with higher volumes and consumption of hydrogen, given the absence of the contribution of alternators, as can be seen in Figure 9.

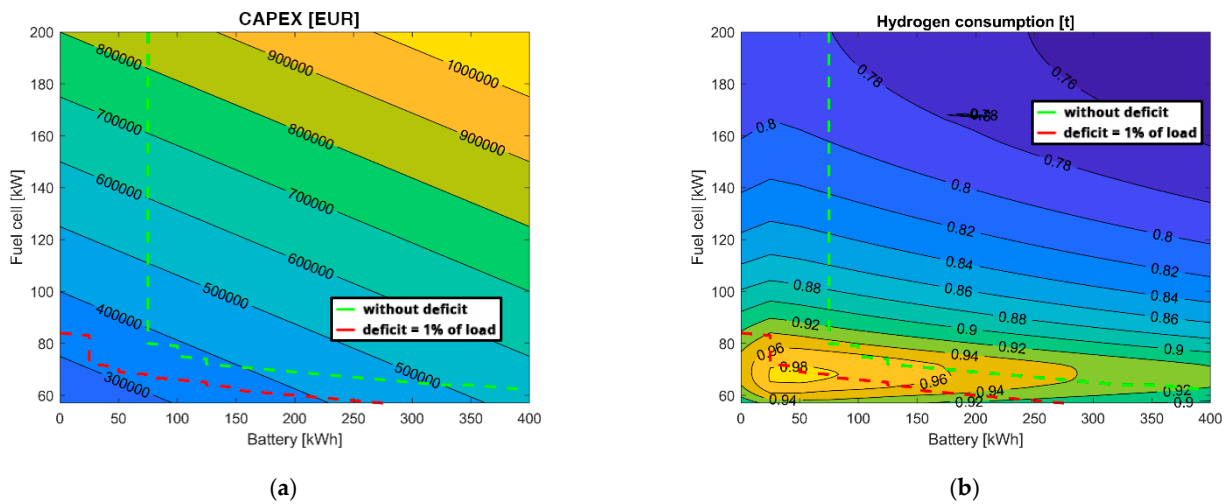


Figure 8. CAPEX (a) and hydrogen consumption (b) of electricity production system of the configuration diesel-hydrogen ICE-FC.

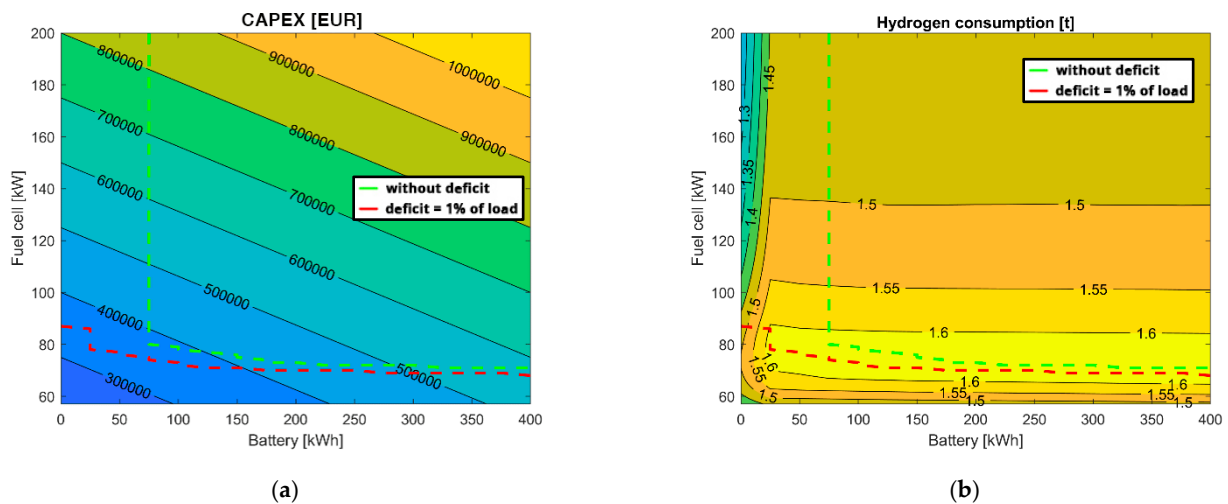


Figure 9. CAPEX (a) and hydrogen consumption (b) of electricity production system of the configuration hydrogen FC.

It is interesting to analyze the data of propulsion with the fuel cell: the CAPEX is 16 times greater than in the use of conventional diesel engines, while the volume occupied by hydrogen is about seven times greater than the baseline. Methanol for propulsion, on the other hand, calculated in the methanol ICE configuration, is 2.5 times more cumbersome than diesel, placing itself halfway between the vectors analyzed from this point of view. From the comparison between the configurations based on the overall volume, in Figure 10, it can be seen how the ICE diesel base case manages to reduce the overall dimensions, followed directly by the synthetic diesel-methanol ICE-FC configuration, which is very interesting.

CO₂ emissions depend on the carbon intensity of the electrical mix [40] used for the synthesis of E-fuels. In Figure 11, a comparison of configurations based on this parameter is shown, with the hypothesis of using the current Italian electricity mix with a specific emission of 258 g/kWhel [41]. At present, the use of synthetic carriers would be counterproductive; for this reason, it is of fundamental importance to increase the adoption of renewable sources in such a way as to decarbonize the sector. A balance would be obtained with specific emissions of CO₂ around 150 g/kWhel.

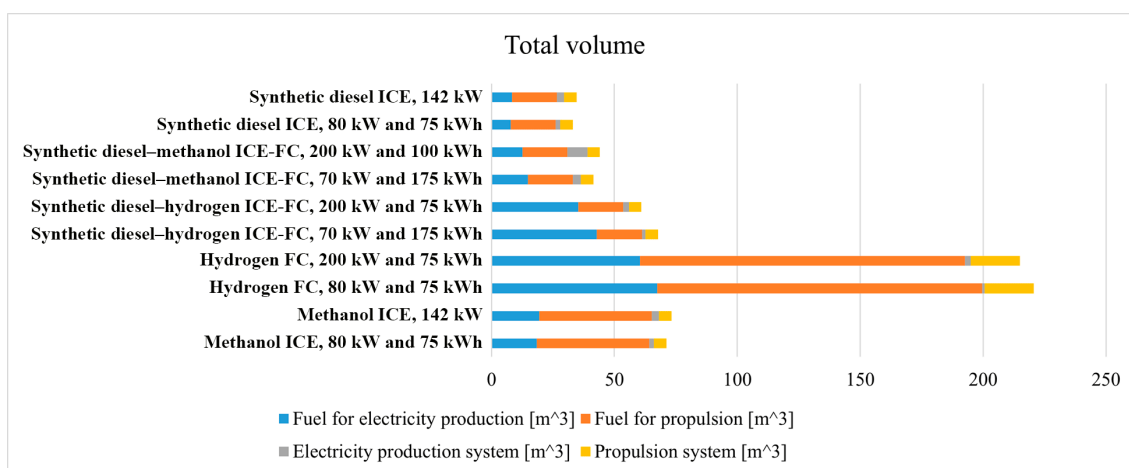


Figure 10. Total volume comparison between configurations.

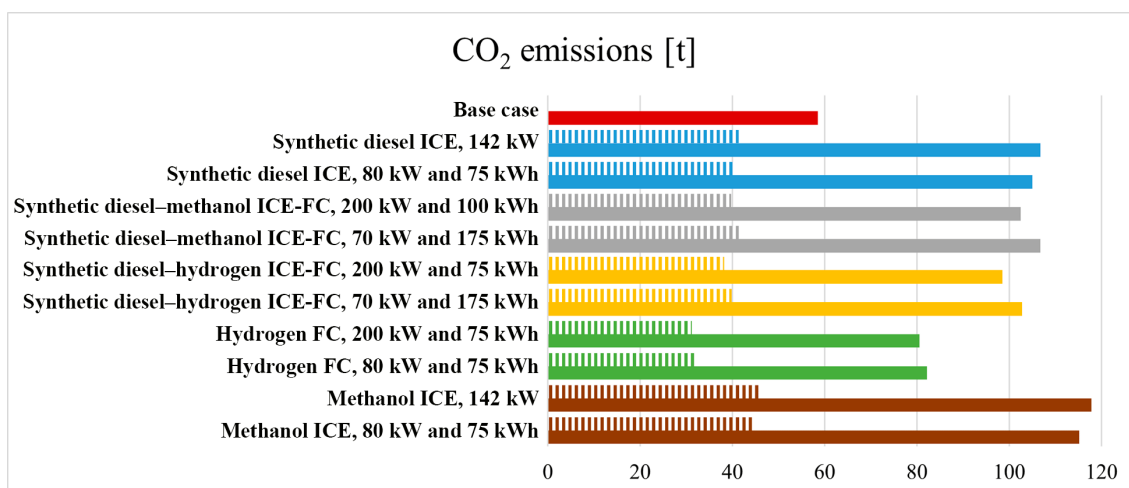


Figure 11. CO₂ emissions comparison between configurations considering a carbon intensity of electricity used for the synthesis of E-fuels of 258 g/kWh_e (solid bars) and 100 g/kWh_e (dashed bars).

5. Conclusions

E-fuels are an option for the decarbonization of some sectors, like pleasure vessels, that cannot be totally electrified. Many onboard layouts are possible. Internal combustion engines and fuel cells can be used with or without electrochemical batteries in hybrid systems to supply onboard electricity and/or boat propulsion.

Compared to an energetic point of view, many pathways, from synthesis to final use, different E-fuels and conversion devices, the result is the absence of a clear winner, suggesting that efficiency (strictly correlated to marginal costs) will not be the key driver.

Pure hydrogen is the worst E-fuel in terms of volume requirements, almost an order of magnitude ($\times 10$) more demanding than the base case. Pure hydrogen is unfeasible for the considered case study. Methanol requires roughly double the volume compared to the current solution, while synthetic diesel (but also biodiesel) is the most straightforward choice because it can directly replace fossil diesel. In fairness, E-fuels and biofuels are competitors in all sectors where direct electrification is not possible, like maritime or air transport, and they should be carefully compared.

In terms of CO₂ emissions, it is important to account for the electricity used for E-fuel synthesis. If the current Italian electricity emission factor is considered (258 gCO₂/kWh_e), E-fuels represent a worsening compared to fossil diesel (+30% up to +100% of CO₂ emissions). With increasing RES penetration in electricity generation, the associated E-fuel emissions will rapidly decrease: the turning point is around 150 gCO₂/kWh_e.

The main limitations of this study are common to similar papers dealing with E-fuels that are very far from market readiness: many assumptions need to be confirmed and updated if real applications are to be available and tested. Sanlorenzo company has planned and launched some experimental campaigns on existing yachts.

Further evaluation must be undertaken regarding the quantity of E-fuels needed each year to decarbonize the whole maritime sector and the associated electricity consumption. With current electricity prices, the cost of E-fuels also represents a significant obstacle that must be studied to understand if there is room for real feasibility.

Author Contributions: Conceptualization, G.P., L.F. and F.T.; methodology, G.P., L.F. and F.B.; validation, G.P., F.B. and F.T.; investigation, G.P. and F.B.; writing—original draft preparation, F.B. and G.P.; writing—review and editing, G.P., F.B., L.F. and F.T.; visualization, G.P. and F.B.; supervision, L.F. and F.T. All authors have read and agreed to the published version of the manuscript.

Funding: The University of Pisa's contribution to this work was partially carried out within the MOST—Sustainable Mobility Center and received funding from the European Union Next-GenerationEU (Piano Nazionale di Ripresa E Resilienza (PNRR)—Missione 4 Componente 2, Investimento 1.4—D.D. 1033 17/06/2022, CN00000023). This manuscript reflects only the authors' views and opinions; neither the European Union nor the European Commission can be considered responsible for them.

Data Availability Statement: The original contributions presented in this study are included in the article. Further inquiries can be directed to the corresponding author.

Conflicts of Interest: Authors Filippo Bollentini and Federico Tocchi were employed by the company Sanlorenzo S.p.a. The remaining authors declare that the research was conducted in the absence of any commercial or financial relationships that could be construed as a potential conflict of interest.

References

1. IMO. International Convention for the Prevention of Pollution from Ships (MARPOL) Annex VI. 1997. Available online: [https://www.imo.org/en/about/Conventions/Pages/International-Convention-for-the-Prevention-of-Pollution-from-Ships-\(MARPOL\).aspx](https://www.imo.org/en/about/Conventions/Pages/International-Convention-for-the-Prevention-of-Pollution-from-Ships-(MARPOL).aspx) (accessed on 12 November 2024).
2. MEPC. IMO Marine Environment Protection Committee. 13–17 May 2019. Available online: <https://www.imo.org/en/MediaCentre/MeetingSummaries/Pages/MEPC-74th-session.aspx> (accessed on 12 November 2024).
3. MEPC. IMO Marine Environment Protection Committee. 7 July 2023. Available online: <https://www.wcdn.imo.org/localresources/en/OurWork/Environment/Documents/annex/MEPC%2080/Annex%2015.pdf> (accessed on 12 November 2024).
4. Mutarraff, M.U.; Terriche, Y.; Niazi, K.A.K.; Vasquez, J.C.; Guerrero, J.M. Energy Storage Systems for Shipboard Microgrids—A Review. *Energies* **2018**, *11*, 3492. [CrossRef]
5. Hardan, F.; Norman, R.; Tricoli, P. Control and operation of a ship AC/DC microgrid under transient propulsion and manoeuvring load conditions. *Int. J. Electr. Power Energy Syst.* **2022**, *139*, 107823. [CrossRef]
6. Nivolianiti, E.; Karnavas, Y.L.; Charpentier, J.-F. Energy management of shipboard microgrids integrating Energy Storage Systems: A Review. *Renew. Sustain. Energy Rev.* **2024**, *189*, 114012. [CrossRef]
7. Zahedi, B.; Norum, L.; Ludvigsen, K. Optimized efficiency of all-electric ships by dc hybrid power systems. *J. Power Sources* **2014**, *255*, 341–354. [CrossRef]
8. Desideri, U.; Giglioli, R.; Lutzemberger, G.; Pasini, G.; Poli, D. Auxiliary Power Units for pleasure boats. In Proceedings of the 6th International Conference on Clean Electrical Power (ICCEP), Santa Margherita Ligure, Italy, 27–29 June 2017.
9. Ferrari, L.; Frate, G.; Giglioli, R.; Girolami, A.; Pasini, G.; Tocchi, F. Feasibility analysis of a hybrid auxiliary power unit for pleasure boats. *E3S Web Conf.* **2020**, *197*, 05005. [CrossRef]
10. Pasini, G.; Lutzemberger, G.; Ferrari, L. Renewable Electricity for Decarbonisation of Road Transport: Batteries or E-fuels? *Batteries* **2023**, *9*, 135. [CrossRef]
11. Ash, N.; Davies, A.; Newton, C. In Renewable Electricity Requirements to Decarbonise Transport in Europe with Electric Vehicles, Hydrogen and Electrofuels. Ricardo Report. 2020. Available online: https://www.transportenvironment.org/uploads/files/2020_Report_RES_to_decarbonise_transport_in_EU.pdf (accessed on 12 November 2024). Ricardo Report.
12. Ampah, J.D.; Yusuf, A.A.; Afrane, S.; Jin, C.; Liu, H. Reviewing two decades of cleaner alternative marine fuels: Towards IMO's decarbonization of the maritime transport sector. *J. Clean. Prod.* **2021**, *320*, 128871. [CrossRef]
13. Keçebaş, A.; Kayfeci, M. Chapter 1—Hydrogen properties. In *Solar Hydrogen Production*; Academic Press: New York, NY, USA, 2019; pp. 3–29.
14. Available online: <https://www.questone.com/en/products/detail/quest-one-pem-electrolyzer-me450/me450> (accessed on 12 November 2024).

15. Sebbahi, S.; Nabil, N.; Alaoui-Belghiti, A.; Laasri, S.; Rachidi, S.; Hajjaji, A. Assessment of the three most developed water electrolysis technologies: Alkaline Water Electrolysis, Proton Exchange Membrane and Solid-Oxide Electrolysis. *Mater. Today Proc.* **2022**, *66*, 140–145. [CrossRef]
16. Hnát, J.; Paidar, M.; Bouzek, K. 5-Hydrogen production by electrolysis. In *Current Trends and Future Developments on (Bio-) Membranes*; Elsevier: Amsterdam, The Netherlands, 2020; pp. 91–117.
17. Sheffield, J.; Martin, K.; Folkson, R. 5-Electricity and hydrogen as energy vectors for transportation vehicles. In *Alternative Fuels and Advanced Vehicle Technologies for Improved Environmental Performance*; Woodhead Publishing: Sawston, UK, 2014; pp. 117–137.
18. Sundén, B. Chapter 3—Hydrogen. In *Hydrogen, Batteries and Fuel Cells*; Academic Press: New York, NY, USA, 2019; pp. 37–55.
19. Jensen, J.; Vestbø, A.; Li, Q.; Bjerrum, N. The energy efficiency of onboard hydrogen storage. *J. Alloys Compd.* **2007**, *446–447*, 723–728. [CrossRef]
20. Meng, X.; Mei, J.; Tang, X.; Jiang, J.; Sun, C.; Song, K. The Degradation Prediction of Proton Exchange Membrane Fuel Cell Performance Based on a Transformer Model. *Energies* **2024**, *17*, 3050. [CrossRef]
21. DNV. Assessment of Selected Alternative Fuels and Technologies. Available online: <https://www.dnv.com/maritime/publications/alternative-fuel-assessment-download/> (accessed on 12 November 2024).
22. Wallner, T.; Lohse-Busch, H.; Gurski, S.; Duoba, M.; Thiel, W.; Martin, D.; Korn, T. Fuel economy and emissions evaluation of BMW Hydrogen 7 Mono-Fuel demonstration vehicles. *Int. J. Hydrogen Energy* **2008**, *33*, 7607–7618. [CrossRef]
23. Bao, L.-Z.; Sun, B.-G.; Luo, Q.-H.; Li, J.-C.; Qian, D.-C.; Ma, H.-Y.; Guo, Y.-J. Development of a turbocharged direct-injection hydrogen engine to achieve clean, efficient, and high-power performance. *Fuel* **2022**, *324*, 124713. [CrossRef]
24. IRENA. Innovation Outlook: Renewable Methanol. 2021. Available online: <https://www.irena.org/publications/2021/Jan/Innovation-Outlook-Renewable-Methanol> (accessed on 12 November 2024).
25. Kauw, M.; Benders, R.M.; Visser, C. Green methanol from hydrogen and carbon dioxide using geothermal energy and/or hydropower in Iceland or excess renewable electricity in Germany. *Energy* **2015**, *90*, 208–217. [CrossRef]
26. Schorn, F.; Breuer, J.L.; Samsun, R.C.; Schnorbus, T.; Heuser, B.; Peters, R.; Stolten, D. Methanol as a renewable energy carrier: An assessment of production and transportation costs for selected global locations. *Adv. Appl. Energy* **2021**, *3*, 100050. [CrossRef]
27. DNV. Alternative Fuels for Naval Vessels. Available online: <https://www.dnv.com/news/dnv-white-paper-tackles-the-decarbonization-of-naval-vessels-219461/> (accessed on 12 November 2024).
28. Wang, Y.; Wu, Q.; Mei, D.; Wang, Y. Development of highly efficient methanol steam reforming system for hydrogen production and supply for a low temperature proton exchange membrane fuel cell. *Int. J. Hydrogen Energy* **2020**, *45*, 25317–25327. [CrossRef]
29. Gribovskiy, A.; Makarshin, L.; Andreev, D.; Klenov, O.; Parmon, V. Thermally autonomous microchannel reactor to produce hydrogen in steam reforming of methanol. *Chem. Eng. J.* **2015**, *273*, 130–137. [CrossRef]
30. IEA. Ammonia Technology Roadmap. 2021. Available online: <https://www.iea.org/reports/ammonia-technology-roadmap> (accessed on 12 November 2024).
31. Rouwenhorst, K.H.; Van der Ham, A.G.; Mul, G.; Kersten, S.R. Islanded ammonia power systems: Technology review & conceptual process design. *Renew. Sustain. Energy Rev.* **2019**, *114*, 109339.
32. DNV. Ammonia as a Marine Fuel. Available online: <https://www.dnv.com/publications/ammonia-as-a-marine-fuel-191385/> (accessed on 12 November 2024).
33. Zhang, H.; Wang, L.; Van herle, J.; Maréchal, F.; Desideri, U. Techno-economic comparison of green ammonia production processes. *Appl. Energy* **2020**, *259*, 114135. [CrossRef]
34. Larsson, M.; Grönkvist, S.; Alvfors, P. Synthetic Fuels from Electricity for the Swedish Transport Sector: Comparison of Well to Wheel Energy Efficiencies and Costs. *Energy Procedia* **2015**, *75*, 1875–1880. [CrossRef]
35. Rödl, A.; Wulf, C.; Kaltschmitt, M. Chapter 3—Assessment of Selected Hydrogen Supply Chains—Factors Determining the Overall GHG Emissions. In *Hydrogen Supply Chains*; Academic Press: New York, NY, USA, 2018; pp. 81–109.
36. Composites, S. 350 Bar Hydrogen. Available online: https://www.hannovermesse.de/apollo/hannover_messe_2021/obs/Binary/A1089958/Steelhead%20Composites%20350%20Bar%20Hydrogen%20Brochure.pdf (accessed on 12 November 2024).
37. van Biert, L.; Godjevac, M.; Visser, K.; Aravind, P. A review of fuel cell systems for maritime applications. *J. Power Sources* **2016**, *327*, 345–364. [CrossRef]
38. Mathworks. How to Decide Window Size for a Moving Average Filter? Available online: <https://it.mathworks.com/matlabcentral/answers/315739-how-to-decide-window-size-for-a-moving-average-filter> (accessed on 12 November 2024).
39. Zhang, R.; Li, X.; Sun, C.; Yang, S.; Tian, Y.; Tian, J.; Zhang, R. State of Charge and Temperature Joint Estimation Based on Ultrasonic Reflection Waves for Lithium-Ion Battery Applications. *Batteries* **2023**, *9*, 335. [CrossRef]
40. Liponi, A.; Pasini, G.; Baccioli, A.; Ferrari, L. Hydrogen from renewables: Is it always green? The Italian scenario. *Energy Convers. Manag.* **2023**, *276*, 116525. [CrossRef]
41. ISPRA. Indicatori di Efficienza e Decarbonizzazione del Sistema Energetico Nazionale e del Settore Elettrico. 2021. Available online: <https://www.isprambiente.gov.it/it/pubblicazioni/rapporti/indicatori-di-efficienza-e-decarbonizzazione-del-sistema-energetico-nazionale-e-del-settore-elettrico> (accessed on 12 November 2024).

Disclaimer/Publisher’s Note: The statements, opinions and data contained in all publications are solely those of the individual author(s) and contributor(s) and not of MDPI and/or the editor(s). MDPI and/or the editor(s) disclaim responsibility for any injury to people or property resulting from any ideas, methods, instructions or products referred to in the content.